ETH
Eidgenössische Technische Hochschule Zürich
Swiss Federal Institute of Technology Zurich

Characterization of cellular enzymatic activity through functional single cell analysis using DropMap

Master's Thesis

Linnea Gidner

Functional Immune Repertoire Analysis Lab

Institute of Pharmaceutical Sciences

Department of Chemistry and Applied Biosciences

Eidgenössische Technische Hochschule Zürich

Supervised by:
Prof. Dr. Klaus Eyer
Dr. Christina Sakellariou

Abstract

Assuming normal distribution within cell populations has long been status quo in cellular research. With the fast development of techniques, numerous examples of heterogeneites within isogenic cultures have been unveiled, demonstrating the need of single cell analysis. Currently there are many widely used techniques for this, such as single cell RNA-sequencing, FACS and CyTOF, allowing high-troughput single-cell genotyping and medium to high troughput single cell phenotyping based on intracellular and cell surface proteins, but not secreted proteins. In this master's thesis project the DropMap technology was utilized to develop high-throughput enzymatic activity assays on a single-cell level, revealing the heterogeneous nature of enzyme secretion and activation, even within cell lines. Around 1500 cells were screened in each assay with the microfluidic technique, providing a precise picture of the cell population and its heterogeneity. Within each assay interesting findings were discovered, such as subpopulations in shape of expression patterns, size and activity levels that could not have been detected in bulk measurements. The importance of activity measurements opposed to only secretion measurements was shown and described. The DropMap technology proved its usefulness both in terms of debug possibilities and explanations but above all its resolution and detailed output, providing a reliable platform for development of highly detailed enzymatic assays on a single cell level.

Introduction

Throughout the history of cellular research most cell studies have relied on an assumption that cells within a defined population are normally distributed [1, 2]. If this assumption is made in a population when it is in fact not normally distributed faulty conclusions can be made. In the review *Dynamic Single-Cell Analysis for Quantitative Biology* by the Lee and Dicarlo research groups [2] some theoretical examples are shown. If the distribution is not Gaussian, but for example as in figure 1a), where a cell population consists of two types of cells creating a bimodal distribution, the average value would in reality not be displayed by any of the present cells, while a gaussian distribution is well characterized by the mean. Indeed, emerging techniques and newly developed methods for single cell analysis have shown that heterogeneities are present in all sorts of cell populations, even when all cells are derived from one mother cell within cell lineages [1, 3, 4, 5, 6, 7, 8]. These heterogeneities differ in size and significance depending on cell type and study, but without a more robust platform with a higher throughput of measuring that heterogeneity the conclusions drawn can be highly misleading. A more complex distribution can only be detected and analyzed on a single cell level.

Numerous techniques have been developed to analyze cells on a single cell level, investigating all different aspects of cell properties [3, 9, 10]. Single-cell RNA sequencing has been advancing considerably the last years and is today a dominant way of studying gene expression at the single cell level [11]. There are multiple droplet-based RNA-seq approaches enabling ultra-high throughput of tens of thousands of individual cells [12]. However, the mediators of most diseases and target of drugs are proteins, not RNA, and the transcriptional profile of a cell will not tell us the specific concentration or location of a protein [13]. Therefore, additional approaches for measuring protein concentration on a single cell level have been developed. A widely used method to analyze cells on a single cell level is fluorescence activated cell sorting (FACS), where single cells are separated by laminar flow focusing. High throughput can be achieved, but only properties such as size, complexity and membrane bound or intracellular proteins can be measured and secreted substances can only be measured indirectly [14]. Time of flight mass cytometry (cyTOF) is another widely used technique to measure protein expression, but also here only membrane bound or intracellular protein can be measured and not secreted protein [15, 16]. Both of these techniques also lack the possibility of kinetic measurements, not revealing the dynamic behavior of cellular populations [17]. Microwells and cell trapping are examples where cells can be analyzed based on surface markers, density or size [18]. Advantages of these approaches are that the cells can be monitored over time and the response in terms of e.g. secretions from a specific cell can be measured. On the other hand, these techniques often have a low throughput, typically less than 10000 cells [3].

In DropMap, a droplet-based microfluidic technique first introduced by Eyer et al. in 2017, many of these limitations are overcome [8]. Here, single cells are captured in 50 pL size droplets creating a highly monodisperse water-in-oil emulsion, where the droplets serve as a microenvironment for the cell as secreted substances are retained within the droplet and can be measured with the use of fluorescent bioassays. Each droplet can therefore function as a well in a microtiter plate, only with a volume almost a million times smaller [19]. In this way the dilution is controlled on a minimized scale, making this method a better option in terms of resolution.

The workflow of an enzymatic assay in DropMap is illustrated in figure 1b, where first the samples are prepared, with one cell solution and one substrate solution. These are then compartmentalized into droplets in a microfluidic device, constructed to produce monodisperse 50 pL size droplets. The device is fabricated in poly-dimethysiloxane (PDMS) using soft-lithography and contains three inlets, one for the carrier oil, one for the cell

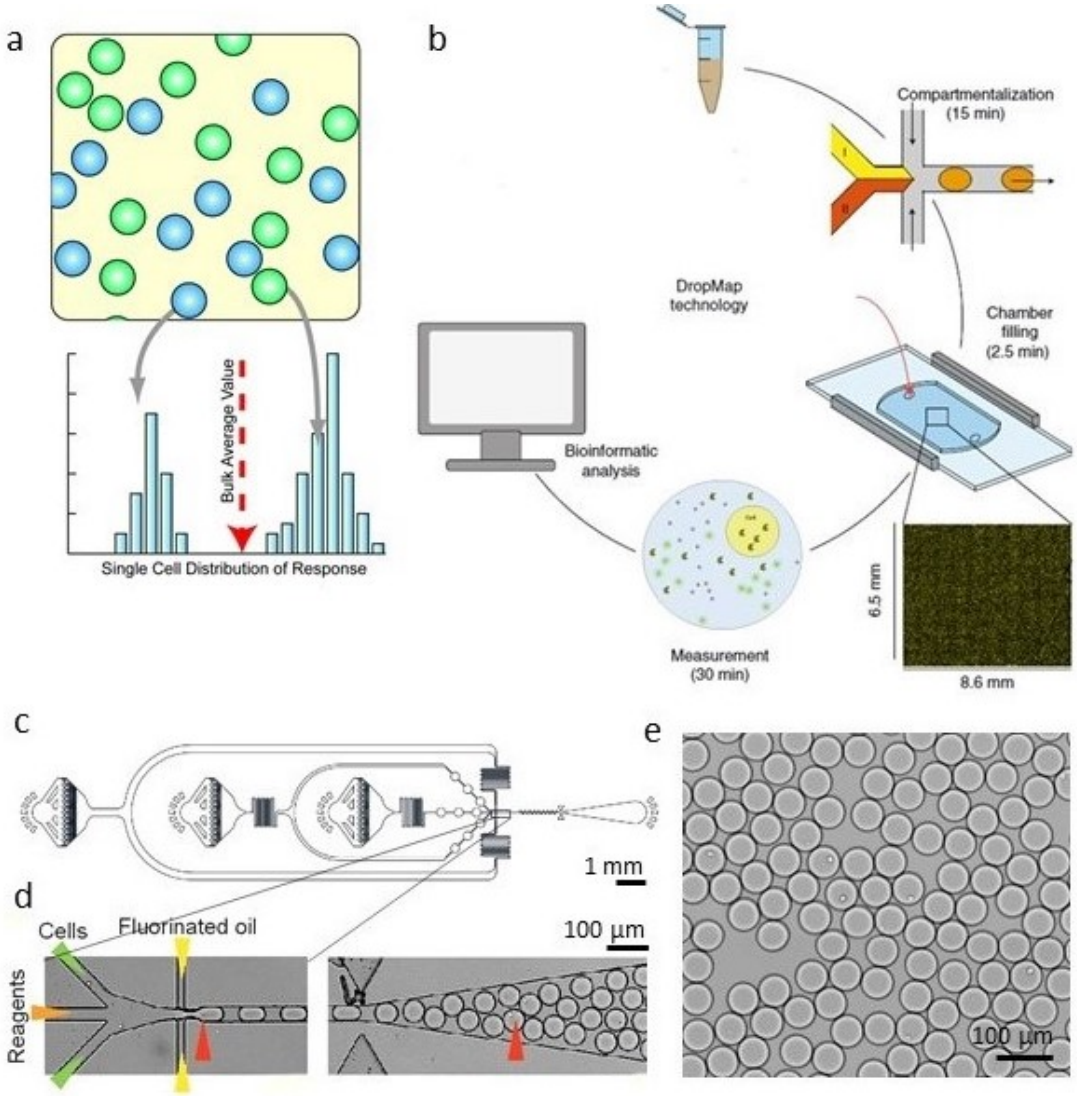

Figure 1: Single cell analysis and the DropMap technology. **(a)** A hypothetical case of a bimodal distribution. Figure taken from [2]. **(b)** Overview of the DropMap workflow. First, the samples are prepared, one aqueous solution with cells and one with the substrate. These are run through a microfluidic chip together with a fluorinated oil creating monodisperse droplets in a w/o emulsion. These droplets are loaded onto an observation chamber with a height slightly smaller than the droplets which immobilizes the droplets and enables measurements over time. The fluorescent signal is measured and the data can be analyzed. **(c)** Enlargement of the microfluidic chip. Oil inlet is the first from left, the next two inlets from left are for the aqueous phases and the outlet is to the right. **(d)** Enlargement of the are where the cells and the assay reagents are co-encapsulated.The red arrows show droplets with cells. Figure taken from [17]. **(e)** A brightfield image of the immobilized droplets in the observation chamber, some containing individual 1D11 cells.

suspension and one for the assay reagents, as well as one outlet (1c and d) [20]. A chip with only two inlets is also available for e.g. calibration curves, where only one aqueous inlet is needed. A fluorinated oil is used as the carrier phase as it can be used with PDMS, it is immiscible with aqueous liquids and transparent (allowing for optical analysis) [21]. A nonionic perfluoro-polyether fluorosurfactant is added to the fluorinated carrier oil to increase the statbility of the droplets [17]. Furthermore, the cells within the droplets can be kept viable for a long time thanks to its oxygen preservation properties. It can dissolve 20 times more oxygen than water, and being both hydrophilic and lipophilic, it is a very poor solvent for organic molecules, hence providing suitable conditions for cell-based assays [20]. After generation of the droplets they are loaded onto an observation chamber, creating a 2D matrix of droplets, constructed with a height slightly smaller than the droplet diameter to immobilize the 50 picoliter droplets. This enables measurements over time, from a few minutes up to 24h [17]. An enlargement of this can be seen in figure 1e. In an area of 1 cm^2 60000 droplets, i.e. around 20000 cells can be captured [17]. The encapsulated cells and their products are then measured under a microscope and the data is analyzed.

This technology has so far been used to characterize antibody-secreting cells in mice immunized with tetanus toxoid, where Eyer et al developed an assay to simultaneously analyze the secretion rate and affinity of IgG from over 0.5 million individual cells [8]. Here, dramatic increases in secretion rates and affinities where observed on a single cell level, whereas the average numbers only increased moderately. DropMap delivered the full picture of the humoral immune response, only possible with a quantitative, kinetic, high-throughput single cell analysis.

The aim of this master's thesis project was to study enzyme secretion and activation on a single cell level using DropMap. The extent of heterogeneity within a cell population will be analyzed and our understanding of secreted enzymes will be deepened. For instance, RNA-seq can reveal whether the cell is able to express the enzyme, but will not be able to localize it, measure the concentration of it or measure if the enzyme is active. By using DropMap to measure the enzyme secretion and turnover, the actual role of a single cell in a greater population can be discovered. As target enzyme, granzyme B was chosen. Granzyme B is together with Granzyme A the most abundant granzyme and has been studied extensively [22]. It is most known to be expressed by cytotoxic T lymphocytes and NK-cells but has been shown to be expressed by a series of other immune cells such as neutrophils, activated macrophages, basophils and dendritic cells [23, 24, 25, 26]. Furthermore, the enzyme is known to induce cell death through the granule pathway [27]. This pathway has been shown to be activated to eradicate pathogen-infected cells and tumors and is therefore often present in cancer and other diseases [28, 29]. If we can understand how this enzyme is secreted by heterogenous primary immune cell populations, this will guide towards deeper understanding of the immune reactions in diseases like cancer and eventually be used in the development of drugs and biomedical and diagnostic applications.

Method and Materials

Cell Cultures

The prostate cancer cell line, LNCaP, the mouse hybridoma cell line, 1D11, the macrophage cell line, RAW 264.7, were used (LGC Standards). LNCaP cells were grown in RPMI-1640 Medium (Thermo Fisher Scientific (Gibco), Waltham, Massachusetts, United States), supplemented with 10% fetal bovine serum (FBS) (GE Healthcare, Chicago, Illinois, United States) and 1% Penicillin-streptomycin (Life Technologies, Carlsbad, California, United States, cat. no. 15140-122). They were grown in a cell culture incubator at 37°C and 5% CO2 in air atmosphere and were passaged 2 times per week using 0.25% (w/v) Trypsin- 0.53 mM EDTA. After detaching the

LNCaP, an additional step of centrifuging the cells at 300 rpm for 5 minutes and discarding of the supernatant was implemented to remove the trypsin from the cell sample. The 1D11 cell line was cultivated by Kevin Portmann according to standard protocol and the RAW 254.7 cell line was cultivated by Professor Klaus Eyer according to standard protocol.

DropMap Workflow

Two methods for droplet gerenation were used. For calibration experiments the droplets were created by hand and for the assays three low pressure syringe pumps neMESYS 290N, and control module Base 120 (both Cetoni, Korbussen, Germany). For this a 200 μL pipette and a microfluidic chip were used. The fabrication of the microfluidic chip has previously been described by Bounab et al [17] and were already premade for this study. When generating the droplets by hand, 200 μL of the fluorinated oil (HFE-7500 oil (3M, Hadfield, UK) containing 0.5% (wt/wt) 008-Fluorosurfactant (RAN Biotechnologies, Beverly, United States) was taken up and placed into the oil inlet of the microfluidic chip. Some of the oil was pushed out until it could be seen in the outlet. The pipette tip was gently released from the pipette and kept in the chip. The aqueous solution was taken up and the tip was placed in the other inlet. Thereafter, an empty pipette tip was placed in the outlet while the plunger button was pressed in. The pipette was placed at a 90°angle to the chip and then the plunger was released. The vacuum in the tip would suck out the liquid and create the droplets. When the pipette tip was filled it was taken out and loaded into the observation chamber. For the system with the pumps, the three syringes were filled with oil, the first with the fluorinated oil and the two second with light mineral oil (Sigma Aldrich). The syringes were mounted on the syringe pumps and the two syringes intended for the aqueous solutions were connected to 200 µL pipette tips using 0.56 mm diameter PTFE microtubing and PDMS slabs (6 mm diameter, with a hole in the middle of 0.75 mm diameter) [17]. These were filled with the light mineral oil and 50 µL of each aqueous solution was taken up. The syringe with the fluorinated oil was connected to the oil inlet of the microfluidic chip and the pipette tips connected to the syringe pumps were placed in the aqueous inlets. The droplets were generated with a flow rate of 200 µL/h of the aqueous phases and either 400 or 800 µL/h depending on the construction of the microfluidic chip. The outlet was connected to the observation chamber with 0.56 mm diameter PTFE microtubing.

A Nikon Eclipse Ti-2E inverted microscope for time-lapse imaging with a 10X magnification was used for the imaging to both be able to detect objects within the droplet and not obtain a too long scanning time. The microscope was equipped with a Perfect Focus System (PFS) that was used to maintain focus throughout the measurement procedure. All measurements included pictures taken in bright field and subsequently in a fluorescence channel depending on the assay.

As previously described, Bounab et al [17] developed a Matlab-based software to detect and track droplets in time-lapse imaging. This software was used to analyze the images taken. The droplets are first detected in bright field images, detecting circles of a certain diameter. Then these detected droplets are analyzed in the other channels for fluorescence in the droplet and the cell.

Flow Cytometry

LNCaP cells were analyzed to ensure production of legumain and MMP-9. LNCaP cells in solution were added to the wells of a 96-well plate for staining (U-bottom). The cells were centrifuged at 1200 rpm for 2 min at 4°C and the supernatant discarded. They were Fc-blocked with blocking α-CD16/CD32 antibody (1 μg IgG/ml: Human or

Marker	Conjugate	Dilution	Manufacturer
LGMN	ALEXA FLUOR® 647	1:100	Bioss
MMP-9	ALEXA FLUOR® 488	1:100	Abcam

Table 1: Single stain controls

Mouse TruStain FcX™, 1:500 in FACS Buffer (containing 1x PBS pH: 7.4, 2.5% FBS and 2mM EDTA)) for 15 minutes on ice and then once again centrifuged at 1200 rpm for 2 min at 4°C and the supernatant discarded. The cells were then incubated with the single stain controls according to table 1 for 20 min on ice. For legumain an isotype control was used and for MMP-9 only the primary antibody was used as control. Dead cells were excluded from the analysis by staining with Zombie Aqua (BioLegend, San Diego, California, United States).

Any unbound antibodies were removed by washing the cells with FACS buffer. The cells were centrifuged at 1200 rpm for 5 min and the supernatant discarded.Then the secondary MMP-9 antibody was added. 2 µL of the antibody were mixed with 400 µL of FACS buffer and then 200 µL were added to each well. The plate was incubated at 4°C in the dark for 20 min. Any unbound antibodies were removed by washing the cells with FACS buffer. The cells were centrifuged at 1200 rpm for 5 min and the supernatant discarded. They were resuspended by adding 200 µL of FACS buffer. This step was repeated two times. The cells were analyzed in the CytoFLEX S Flow Cytometer (Beckman Coulter; 4 lasers, 13 colors) with the use of CytExpert software. The data was analyzed in FlowJo v10.6.2.

Calcein Red-Orange AM Experiments

A sample of cells from a mouse hybridoma cell line 1D11 was collected and centrifuged. The supernatant was discarded and PBS was added to reach 3 million cells/mL. To this solution 5 μM cell trace violet (ThermoFisher Scientific, cat. no. C34557) was added. The sample was incubated at 37°C for 10 min while a calcein red-orange AM (ThermoFischer Scientific) solution of 5 μM was prepared in PBS. The cell sample was centrifuged and the supernatant discarded. PBS was added to achieve a concentration of 6 million cells/mL for encapsulation. The pumps were prepared with the solutions and then the droplets were created and analyzed. Measurements were performed in bright field and fluorescence was measured at excitation and emission wavelengths of 358 nm and 461 nm (DAPI filter), as well as 577 and 590 nm (mCherry filter) every 10 minutes for 1 hour, for overview see table 2. This experiment was repeated six times.

MMP Activity Assay

The MMP secretion and its turnover from LNCaP cells were measured in the droplets. LNCaP cells were detached with trypsin EDTA, collected in a centrifuge tube and centrifuged. The supernatant was discarded and PBS was added to reach 2 million cells/mL. Cell trace violet was added and the solution was incubated at 37°C for 10 minutes and then centrifuged for 5 minutes at 300 rpm. During that time the substrate/activation solution was prepared. 4-Aminophenylmercuric Acetate (APMA) and MMP green substrate (both Abcam, Cambridge, United Kingdom) were diluted in cell buffer containing RPMI 1640 with Glutamax (w/o phenol red) (Thermo Fischer Scientific) supplemented with 10% KnockOut Serum Replacement (vol/vol) (Thermo Fischer Scientific), 1x Penicillin-streptomycin, 0.1% Pluronic F-127 (Thermo Fischer Scientific), 0.5% (w/v) rHSA (Sigma Aldrich) and 25 mM HEPES (Thermo Fischer Scientific), at a ratio 1:500 and 1:100 respectively. The fluorescence was

measured at excitation and emission wavelengths of 358 nm and 461 nm (DAPI filter), as well as 490 and 525 nm (FITC filter) every 10 minutes for 2 hours, for overview see table 2. This experiment was repeated three times with APMA and three times without.

Lysozyme Activity assay

The lysozyme secretion and its turnover from RAW cells were measured in the droplets. A sample of RAW cells was collected through scratching them of the surface, added to a centrifuge tube and centrifuged for 5 minutes at 300 rpm. The supernatant was discarded and PBS was added to reach 2 million cells/mL. Calcein red-orange AM was added and the solution was incubated at 37 for 10 minutes and then centrifuged for 5 minutes. During that time the substrate solution was prepared. 4-Methylumbelliferyl β-D-N,N',N"-triacetylchitotrioside (Sigma Aldrich) was diluted in cell buffer at a ratio 1:500 and 1:100 respectively. The fluorescence was measured at excitation and emission wavelengths of 577 and 590 nm (mCherry filter), as well as 358 nm and 461 nm (DAPI filter), every 10 minutes for 1 hour, for overview see table 2. This experiment was repeated three times.

Channel	**DAPI**	**mCherry)**	**FITC**
Esterase	Cell detection	Kinetic measurement in cell	–
MMP	Cell detection	–	Kinetic measurement in droplet
Lysozyme	Kinetic measurement in droplet	Cell detection	–

Table 2: Overview of experiments

Results

Measuring granzyme activity on a single cell level from primary cells was expected to give results with a high heterogeneity. This would make the result difficult to reproduce and without a calibration of the assay, the heterogeneity could not be proved to originate from the cells. Therefore, more homogeneous systems were tested in the beginning, using cell lines that, at least in theory, would generate a more homogeneous result. Several systems were considered, and experiments on 1D11 cells with calcein were started as the first and simplest system. Then, LNCaP cells were analyzed for both the enzyme legumain and matrix metalloproteinases (MMP) in a FACS analysis and we chose to proceed with the MMP measurements. Unfortunately, the circumstances around COVID-19 closed down the research facilities in Switzerland for several weeks which forced an interruption of the experiments. This delayed both the working process and also no human blood could be ordered, which made it impossible to include primary cells in this study. Therefore, a new final system was chosen. The macrophage cell line RAW 264.7 was used, performing an activity assay targeting lysozyme. This system was expected to complement the two prior systems (esterases in 1D11 cells and MMP from LNCaP cells) in terms of a greater heterogeneity and complexity.

Cell encapsulation

The assays were based on the DropMap technology, where cells are co-encapsulated with the assay reagents in a water in fluorinated oil emulsion by hydrodynamic flow focusing in a microfluidic system [8]. The aim is to obtain as many droplets with one single cell and as few as possible with multiple cells. The number of cells encapsulated

within one droplet should in theory follow a Poisson distribution. In these experiments a λ of 0.2 was aimed for, where 82% of the droplets are empty, 16% contain one cell and only 1.8% contain multiple cells. However, in most of the experiments the cells to some extent adhered to each other, requiring some further dilution, yielding results with around 15000 measured droplets where around 1500 contained cells. It is possible to measure considerably larger numbers [8, 17], but for this study higher numbers were not considered necessary, especially since this would generate much larger data files.

Calcein Red-Orange AM experiments

The first and simplest system was using the cell-viability dye calcein red-orange AM on a 1D11 hybridoma cell line. Calcein red-orange, AM is a highly lipophilic dye that enters viable cells and is cleaved to red fluorescent (590 nm) calcein red-orange by esterases within the cell (figure 2a) [30]. In this case, the cleaving enzyme (the esterase) was not secreted by the cell and the system therefore only displayed the kinetics of turnover rate. The average of the normalized cellular fluorescence from each individual cell from three replicates can be seen in figure 2b (on average 1370 cells were measured in each replicate). A number of representative single cells are displayed in the same graph to illustrate the heterogeneity within the cell population of the cell line. The distribution of the fluorescence increase over time (i.e. the slope calculated with linear regression) from four different replicates is shown in figure 2c. All the distributions were tested for normal distribution with D'agostino and Pearson omnibus K2 test in GraphPad Prism. None of them passed the normality test, even when outliers were removed. The lock-down of the research facilities in Switzerland during the time period of the project caused a necessity to freeze and defreeze cells creating inconsistency in the technical replicates. This however, could be tracked in the results since the resolution of the single cell analysis allows to detect subpopulations and explain the difference of the result, proving the repeatability of the assay. Even though the distributions were shown not to be normally distributed, they were fitted to a Gaussian distribution, as this was considered a good approximation and a convenient way to analyze the data, values shown in table 3. The Gaussian fit of the replicate 2 days after defreeze is 0.78 and it can clearly be seen that this population is not following a Gaussian distribution. The further away from the defreeze the experiments are conducted, the better the fit gets with an R squared value of 0.85 at 7 days after defreeze and then 0.95 both at 11 days and >30 days after defreeze. The mean of the distribution was highest at 2 days after defreeze at 0.043$\pm$0.093 /min. The mean then lowered, on 7 days after defreeze it was 0.013$\pm$0.188 /min and thereafter increased slightly moving further away from the defreeze day, with a mean of 0.018$\pm$0.265 /min at day 11 after defreeze and 0.021$\pm$0.027 /min at >30 days after defreeze. At day 7 after defreeze a subpopulation can be detected in the histogram where the fluorescence increase was 0.

Days since defreezing of cells	**>30**	**11**	**7**	**2**
R squared	0.95	0.95	0.85	0.78
Amplitude	4.99	4.07	2.57	3.21
Mean	0.016	0.008	0.013	-0.008
Standard deviation	0.007	0.009	0.015	0.008
Coefficient of variation	0.45	1.08	1.17	1.11

Table 3: Gaussian fit values

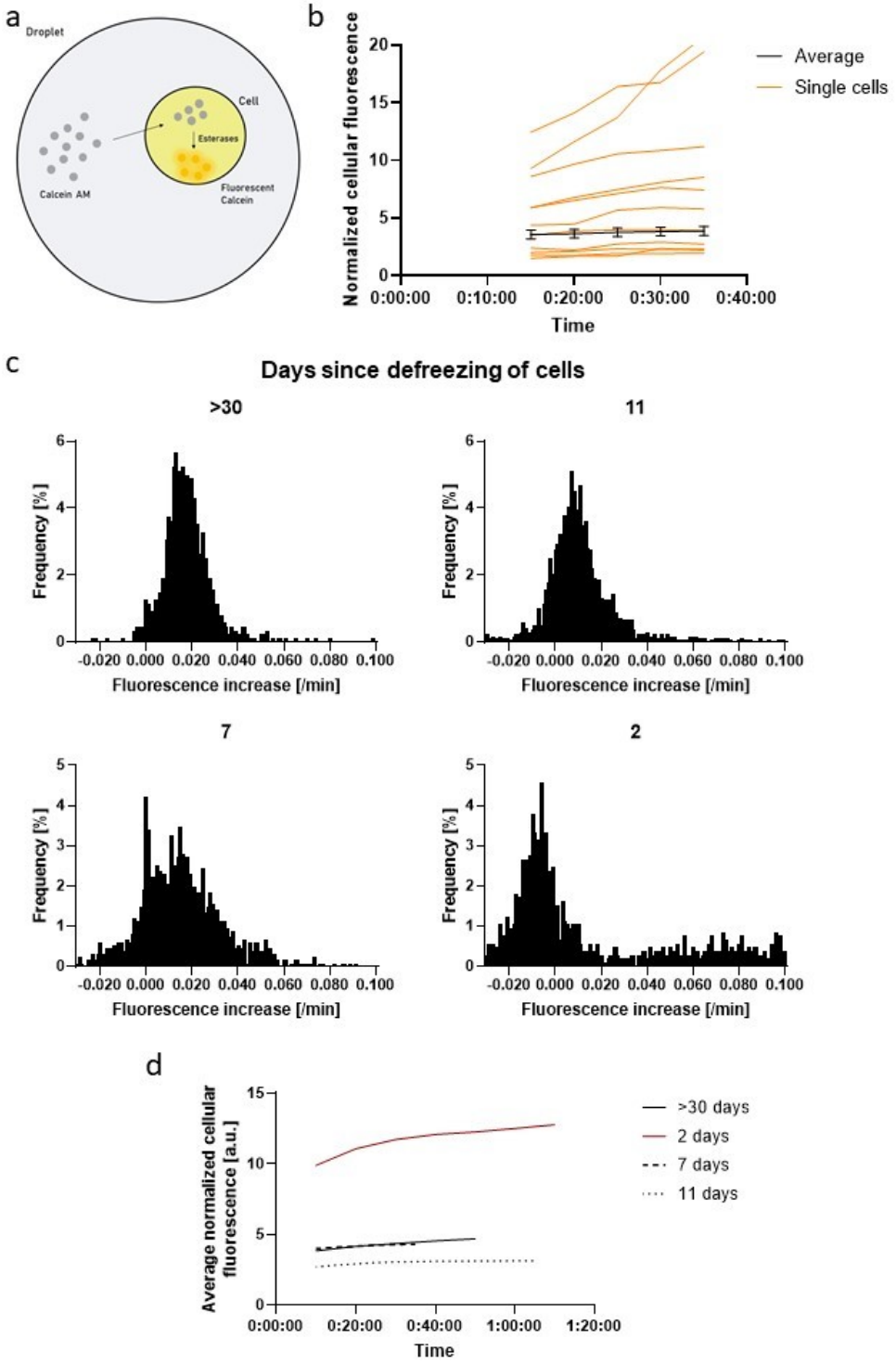

Figure 2: Single cell calcein red-orange assay. **(a)** A schematic illustration to describe the biochemical reaction within the droplet containing cells. The lipophilic calcein red-orange, AM enters the cell and esterases cleave it to red fluorescent calcein that cannot leave the cell. **(b)** The increase of cellular fluorescence over time. The average over all cells is shown in black with error bars representing the standard error from three replicates, and single cells picked at random shown in orange. **(c)** Distribution of the fluorescence increase (/min) of all single cells in the population. The histograms are labeled depending on when the cells in each experiment were defreezed.

MMP activity assay

The second system was measuring the activity of MMP expressed in LNCaP cell. The flow cytometry analysis was performed using a specific antibody against MMP-9. The gating strategy of the analysis can be seen in figure 3. FSC-A vs SSC-A gating selected for cells and sorted away debris (a). Single cells were selected with SSC-A vs SSC-H gating (b). Live cells were then selected based on the exclusion of nonviable cells using Zombie Aqua staining (c). In figure 3(d) and (e) the gate for MMP9+ can be seen, made both on the control and the MMP9+ sample. Comparing e) and d) it can be seen that the LNCaP cells express MMP-9. In (f) this is illustrated with a histogram and the geometric mean with a value of 38422 for the MMP+ sample versus 9922 for the control sample. This only tests the membrane expression of MMP-9, which means that a bigger part of the population also could express MMP-9 intracellularly.

In this assay, the cells either expressed MMP on the membrane or secreted MMP (figure 4a) adding some complexity for the data analysis. Three experiments of the assay were performed with APMA, known as an MMP activator [31, 32, 33] and three experiments were done without. The two first results with APMA showed a lower response than the experiments without APMA, but the third one was in the same range as the experiments without APMA. However, when the second experiment with APMA was performed it was noticed that the APMA had fallen out in the aqueous solution. This was closely observed in the third experiment, here the APMA was completely solubilized. The first two experiments with APMA were therefore excluded, as it could not be said with certainty what they included and what not. In figures 4c and d, the distributions of the fluorescence increase without APMA respectively with APMA are shown. Here it can be seen that the experiment with APMA had a higher response than the one without. A two-tailed t-test was performed, with a threshold set to $P<0.01$ generating a result of the two distributions being statistically significant, the mean of the experiment with APMA was 83 ± 67 a.u./min, the mean of the experiment without was 29 ± 26 a.u./min. The fluorescence increase distributions from the three experiments without APMA were analyzed with a one way ANOVA test which showed no statistical significant difference between them, with a p value of 0.1108. These three tries with APMA had means of 56 ± 26, 51 ± 33 and 29 ± 22 a.u./min., which could be led back to the fact that all the cell lines had to be thawed again after the reopening of the lab. The results were therefore compared from how much time that had elapsed since they were defreezed. All the distributions were tested for normal distribution with D'agostino and Pearson omnibus K2 test in GraphPad Prism, where only the distribution from the experiment 5 days after defreeze passed the test with a p value of 0.93. One day later, at 6 days after defreeze the distribution was not normal anymore, with a p value of 0.0024 and the one from day 7 after defreeze was also not normal, with a p value of <0.0001.

Lysozyme activity assay

The final assay performed was measuring the activity of lysozymes from the macrophage cell line RAW 264.7. An illustration of this system is shown in figure 5a. The hypothesis was that the lysozyme would be secreted and catalyze the reaction in the droplet, as in B in figure 5a [34]. However, the results implicated something else. Firstly, only 10% of the cells showed an increased signal compared to the empty droplets in the lysozyme channel (figure 5b). Interestingly enough, these cells did not show an increased signal compared to the empty droplets from the calcein red-orange that they were marked with before the encapsulation. Secondly that signal was very strong from the cell itself and although the droplet had a somewhat higher signal compared to the empty droplets (on average 5 times higher), there was no clear sign of an increase in signal within the droplets during the time period

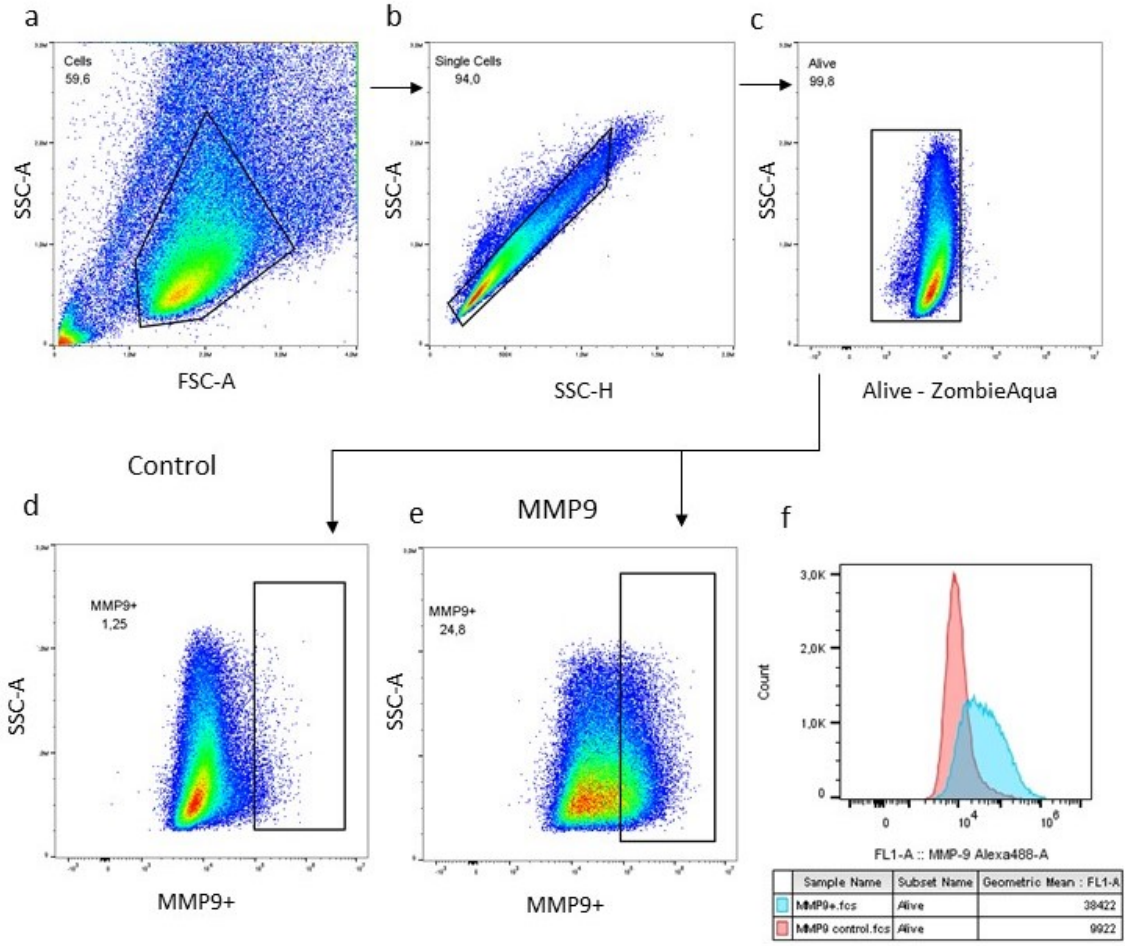

Figure 3: Gating strategy as performed with flow cytometry. (**a**) A gate for cells was set with FSC-A vs SSC-A. (**b**) Single cells were gated based on SSC-A vs SSC-H gating. (**c**) Dead cells were excluded with a gate using Zombie Aqua staining. (**d**) A gate for the MMP9+ cells was set up with Alexa Fluor 488 in both the control (**e**) and with the cells with antibodies for MMP9. (**f**) Histogram showing the control and the MMP9+ cells and the geometric mean.

of measurement. This can be seen in figure 5c, where only the the droplets with the cells that are lysozyme positive are shown. Also figure 5d, the distribution of the fluorescence in the droplets, shows only the droplets with the lysozyme positive cells where 80% of the droplets with lysozyme positive cells have a fluorescence at 2000 a.u.. Yet the mean over all droplet was 5003$\pm$7875 a.u. caused by a few cells with a drastically higher fluorescence. Thirdly, when observing the cells in the bright field channel it was clear that the lysozyme positive cells had a bigger diameter than the other cells and that they did not show any characteristics of apoptotic or dead cells.

Discussion

In this master's thesis intracellular and extracellular enzymatic activity was studied on a single cell level. Different cell-enzyme systems were used generating several occasions where the DropMap technology proved its usefulness in terms of the possibility to track data points back to the images taken. For each system, interesting observations could be made and when the data was not fully consistent the possibility of going back to the original images taken proved itself very useful.

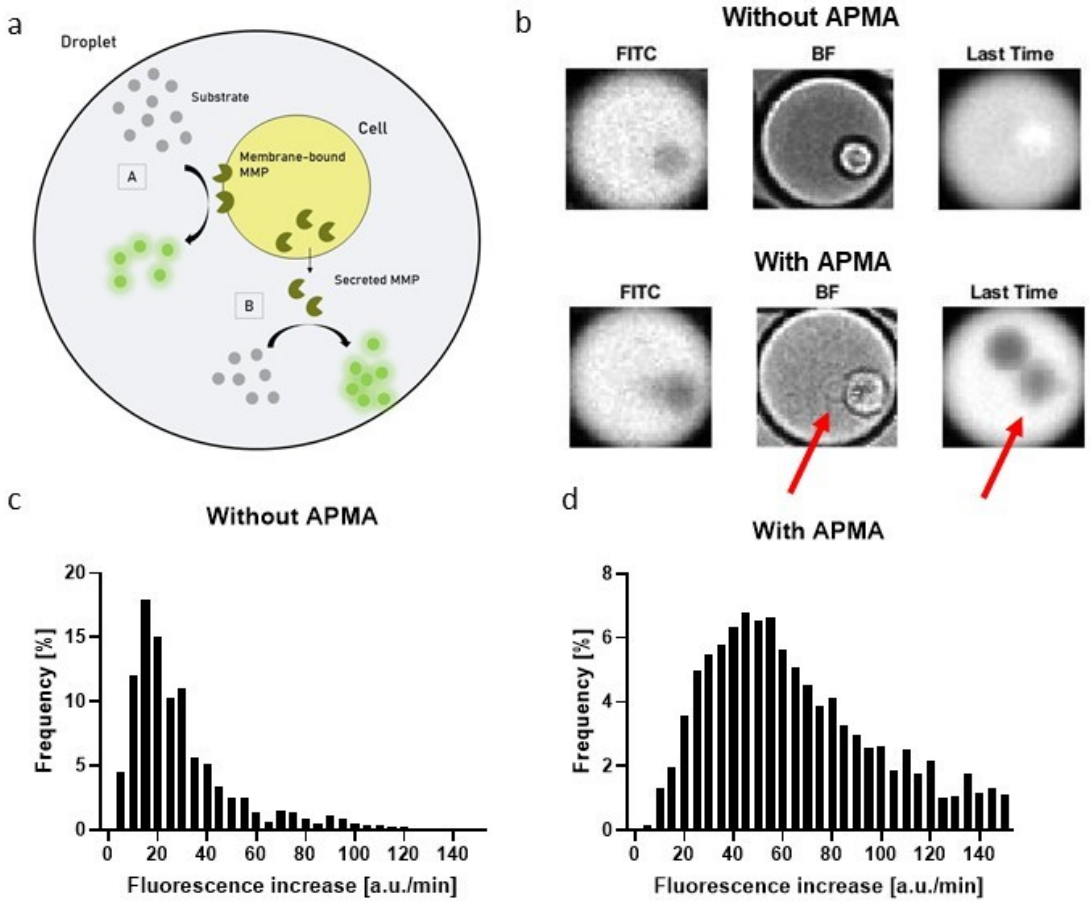

Figure 4: MMP activity assay. (**a**) A schematic illustration to describe the biochemical reaction within the droplet containing cells. The substrate could either be cleaved by membrane-bound MMP (A) or by secreted MMP (B). (**b**) Three images of the same droplet from a experiment without APMA and three images of the same droplet from a experiment with APMA. The one to the left is FITC channel from first time point and the one in the middle in the bright field channel from **continue**. The picture to the right is from the last time point in the FITC channel. Here it can be seen that the cell membrane starts to bulb out from the cell in the one with APMA, already a small bulb in the two first images and a bigger in the last image to the right. This can be compared with the images from the experiment without APMA. (**c**) Distribution of the fluorescence increase in the droplet (a.u./min) of all single cells in the population from a experiment without APMA. (**d**) Distribution of the fluorescence increase in the droplet (a.u./min) of all single cells in the population from a experiment with APMA.

The problems caused by the lock-down of the lab provided an opportunity to prove the robustness of the DropMap technology. The results from the calcein experiments varied from before and after they were freezed, but this could be tracked in the distribution histograms with the findings of subpopulations at an fluorescence of 0, and therefore be explained as the apoptotic cells. Although calcein red-orange AM is a viability dye, it will in some extent color the cells that have a leaky membrane and still functioning esterase production. This subpopulation could even be roughly compared to the cell count with trypan blue, that showed around 50% dead cells for all the replicates done within 11 days of the defreezing. If the apoptotic cells are estimated from the histograms also a number around 50% is obtained. This subpopulation causes the amplitude and mean to decrease, seen in table 3. This subpopulation also mean that there are two ditributions within one, which might be why some of the distributions did not pass the test for normal distribution. Another reason could be that there is a tail to the right on all the curves, cells that have a drastically higher esterase activity. It might be worth to notice that the two first distributions (<30 days and 11 days) have a more normal distributed shape, with the Gaussian

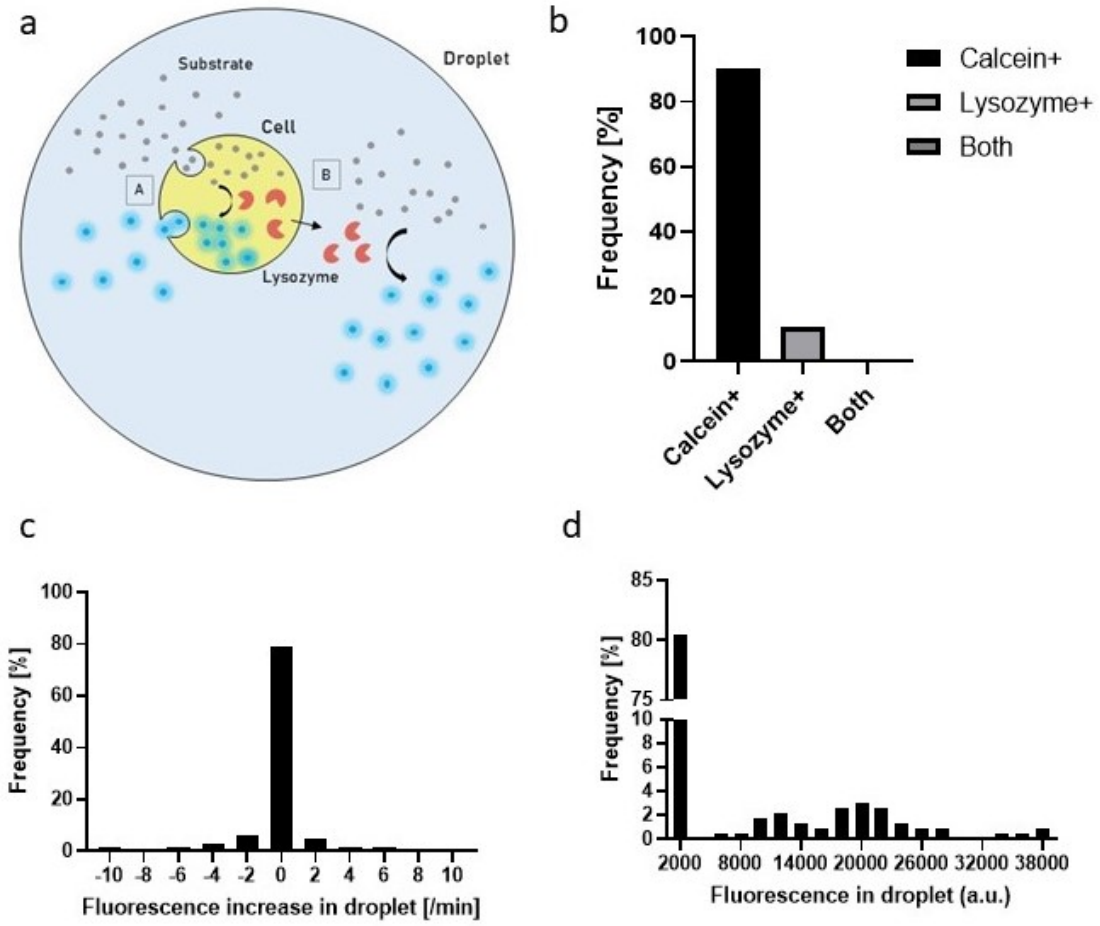

Figure 5: Lysozyme activity assay. The data shown is from one experiment. (**a**) A schematic illustration to describe the biochamical reaction within the droplet containing cells. (**b**) Frequency of cells marked with calcein red-orange and cells with a signal from the dye in the lysozyme assay. The ones that were calcein positive had no signal from the dye and the other way (**c**) Distribution around.of the fluorescence increase (/min) of all single cells in the population. (**d**) Distribution of the fluorescence in droplet (a.u.) of all single cells in the population

fit of these curves having a very high R squared value, whereas it is very clear to the observer that the two later distributions (7 days and 2 days) are not at all normally distributed. The data and most of all the average of the lower right histogram in figure 2c, where the cells had only been thawed for two days, was unexpected. Here, the apoptotic cells no longer only make out a small subpopulation, but they are the visibly bigger population. The extremily heterogenous subpopulation to the right in the histogram are the viable cells. The most striking though are the numbers, the average fluorescence is around three times higher than for the other replicates. This could be explained by a destabilization of the cell membrane, causing higher concentrations of calcein AM to enter the cell or an altered esterase production when thawing the cells, as has been showed before [35]. If these experiments would have been made in bulk only the average fluorescence would have been obtained as in figure 2d. Here, the apoptotic cells would have been hard to make out and especially the experiment just two days after defreezing of the cells could have been interpreted in a very different way.

In the MMP attempts, a higher fluorescence increase in the experiment with APMA, the MMP activator, could be observed, with a mean value almost three times higher than in the experiment without APMA. It can be assumed that a similar amount of MMP is secreted in both attempts, but that all MMP is simply not activated in

the experiment without the APMA, suggesting that two thirds of the MMP is not activated without adding APMA. This is why it is not only important to study secretion of enzymes, but the actual activity.

Additional interesting observations were made when observing the images of the cells in the experiment with APMA. Figure 4b shows two figures each containing three pictures of the same droplet, one of the figures from an experiment without APMA and the other from the experiment with APMA. The picture to the left is taken in the FITC channel and the one in the middle is taken in the brightfield channel, both from the first measured time point. The picture to the right is from the last measured time point in the FITC channel. In the picture from the APMA experiment, it can be seen that the cell membrane starts to bulb out from the cell, already a small bulb at the first measured time point, and a bigger in the last image to the right. This can be compared with the picture where no APMA was used, displaying a normal shape of the cell throughout the experiment. This phenomena was recurring in several droplets with cells in the APMA experiment, suggesting that the APMA affects the cell membrane in an unknown manner. For this reason, APMA should in future studies be used with care together with cells.

No significant difference between the three attempts without APMA could be observed, which is what can be expected. However, the p value of 0.11 means that the probability of obtaining a result with that big differences when the replicates are from the same population is 11%, i.e. the difference was still quite high. This can be explained partly with the different time span since defreeze, but partly also because of the sample size (in these three attempts on average around 500 cells). Since the sample size is so high, the statistical calculations will have a much higher probability of showing significant difference. A perfectly performed replicate should not be different, but the slightest change of procedure will lead to a statistically dramatic change.

Comparing the means of the distributions of the experiment without APMA, it is interesting to see that the closer to the defreeze the experiment was made, the higher activity is. From day 5 to day 7 the average fluorescence increase has decreased with 48%. This is the same phenomena that was seen in the calcein experiments where the average esterase activity was strikingly higher closer to defreeze than when the culture has had some time to establish. Another aspect that could contribute to this high signal closer to the thawing of the cells is that the dye used in the MMP experiments is a more general dye that could potentially have been cleaved by other active peptidases that are more active when the cell has recently been thawed.

The DropMap technology provides an impressive possibility to debug with the help of the images that the data is generated from. One MMP experiment turned out with a considerably higher signal than the others. When the images were analyzed, it could be seen that also the droplets without any cells showed an increase in signal. The conclusion was that some of the medium containing secreted MMP had not been washed away, hence giving a higher signal in both droplets without cells and in droplets with cells. This both explained the higher signal and showed that the medium contained already secreted and active MMP. This experiment would of course have to be repeated to prove this theory.

The unexpected results of the lysozyme assay invited to another theory of what was taking place within the cell containing droplets. Instead of lysozyme secretion, the cell could be utilizing pinocytosis, taking up some substrate, cleaving it inside the cell, and then exchanging some of the product with the outside. Consequently, the cellular fluorescence would be much higher than the average fluorescence in the droplet as could be seen in the obtained results. This is also the case when observing the distribution of the fluorescence increase in the droplet, where most of the droplets containing blue-fluorescent cells don't have a fluorescence increase. This could mean that when the measurement was done, the reaction was already over and what we see is purely the result after the reaction. However, in figure 5d we can see that some droplets had a higher signal. This could mean that in the whole

population around 10% (figure 5b) express lysozyme. Out of these cells the majority keep the lysozyme within the cell, potentially because there was no external stimuli initiating the secretion of lysozyme. A small portion (figure 5d) however, where spontaneously activated and hence secreted the lysozyme, generating the results with around 20% of the droplets containing lysozyme positive cells, with around ten times higher fluorescent signal. This experiment was repeated three times and the amount of cells with a fluorescent signal in the DAPI channel appeared to be similar in the second and third. However, in both of these attempts the blue-fluorescent cells adhered to each other and resulted in the same droplets. This suggests that these cells had a higher probability of adhering and might be a consequence of certain activation. The fact that the cells that were lysozyme positive were not calcein red-orange positive and vice versa can have several explanations. The lysozyme positive cells might for instance express transporter proteins like the multidrug resistance protein [36] that transports the calcein out of the cell again. This experiment illustrates how DropMap provides us with a picture of a more complex system with much higher resolution than if the assay would have been executed in bulk.

The capability of DropMap to genereate such great resolution provides the researcher with an enormous amount of data to work with. This can be overwhelming, from bulk measurements only an average result is obtained and can at times be more handy to interpret, especially for the less skilled researcher. But with the right knowledge and experience, the massive amount of information obtained from experiments with DropMap can be investigated and interpreted to more accurate and more detailed explanations of what is actually happening.

The overall conclusion of the assays in this master thesis project is that the heterogeneity within a cell population is bigger and more complex than normally assumed. Not even the most simple experiments with calcein AM could be proven to be normally distributed. However, cell populations being heterogeneous has been known for a long time, what DropMap contributes with is the ability to characterize and quantify these heterogeneities. This equips the researcher with a powerful tool, pointing at the aspect of interest, providing a more precise picture of the system of interest.

To continue the work that was done in this project, further experiments on the MMP assay and lysozyme assay could be performed. The effects of APMA on the cells could be investigated as well as further measurements of the secretion versus turnover kinetics. It would be interesting to quantify the secretion of MMPs and be able to draw a conclusion between how much MMPs that are secreted and how much that is membrane bound. Furthermore, examining the activity of one specific MMP, like MMP-9, could show a more detailed picture of the heterogeneity. The way that the assay is currently designed it might be that the heterogeneity in a cell population considering one specific MMP is outweighed with the herogeneity of another MMP and the result is therefore more homogeneous. Moving over to the lysozyme activity assay, firstly further replicates of the assay would have to be done to establish the ratio of lysozyme positive cells and deeper investigate the adhesive nature of these cells. Subsequently an external stimulus could be added to the assay to observe the possible increase in lysozyme production and secretion. To proceed further, an enzymatic activity assay with primary cells could be developed to investigate the heterogeneity and quantify the difference between a cell line and primary cells. The information gain that these studies will lead to, can help improve the knowledge of all the enzymatic activities keeping up life, like digesting food, muscle and nerve function, and respiration just to name three out of thousands of functions. It will also help us improve the treatments of enzymatic disregulations, like blood clotting, or to circumvent metabolic enzymes expressed by cancer cells that affect the ability of immune cells to infiltrate tumors.

Acknowledgements

First and foremost I would like to thank Prof. Dr. Klaus Eyer, both for giving me the opportunity to work on this fascinating project and for his supervision and support throughout the whole project. I would like to express my gratitude for the privilege to work with a cutting-edge technology like DropMap, and for showing me innumerable ways of utilizing its high throughput and resolution.

Also, I am deeply grateful for the support from Dr. Christina Sakellariou who was always available whenever I had questions and for encouraging me throughout the project.

I would also like to thank Olivia Bucheli, Kevin Portmann and Ingibjörg Sigvaldadottir for the warm welcome to the group and always keeping a positive vibe while working. Thank you Olivia, for teaching me several cell culture techniques and showing me around in the lab on the first days. Thank you, Kevin and Inga, for introducing me to the microfluidics of droplet creation with the DropMap technique. And thank you all for helping me whenever I had questions or was in doubt.

Further I would like to express my gratitude to Claudia A. Castro Jaramillo for introducing me to flow cytometry and guiding me through different assays.

Lastly, I would like to express a special gratitude to Alexander Johansen for his support and understanding during the long days of home office during the project.

References

[1] Haakan N Joensson and Helene Andersson Svahn. Droplet microfluidics—a tool for single-cell analysis. *Angewandte Chemie International Edition*, 51(49):12176–12192, 2012.

[2] Dino Di Carlo and Luke P Lee. Dynamic single-cell analysis for quantitative biology, 2006.

[3] Lucas Armbrecht and Petra S Dittrich. Recent advances in the analysis of single cells. *Analytical chemistry*, 89(1):2–21, 2017.

[4] John L Spudich and Daniel E Koshland. Non-genetic individuality: chance in the single cell. *Nature*, 262(5568):467–471, 1976.

[5] Tim J Strovas, Linda M Sauter, Xiaofeng Guo, and Mary E Lidstrom. Cell-to-cell heterogeneity in growth rate and gene expression in methylobacterium extorquens am1. *Journal of bacteriology*, 189(19):7127–7133, 2007.

[6] Alejandro Colman-Lerner, Andrew Gordon, Eduard Serra, Tina Chin, Orna Resnekov, Drew Endy, C Gustavo Pesce, and Roger Brent. Regulated cell-to-cell variation in a cell-fate decision system. *Nature*, 437(7059):699–706, 2005.

[7] Alan Diercks, Heather Kostner, and Adrian Ozinsky. Resolving cell population heterogeneity: real-time pcr for simultaneous multiplexed gene detection in multiple single-cell samples. *PloS one*, 4(7), 2009.

[8] Klaus Eyer, Raphaël CL Doineau, Carlos E Castrillon, Luis Briseño-Roa, Vera Menrath, Guillaume Mottet, Patrick England, Alexei Godina, Elodie Brient-Litzler, Clément Nizak, et al. Single-cell deep phenotyping of igg-secreting cells for high-resolution immune monitoring. *Nature biotechnology*, 35(10):977, 2017.

[9] Christian Dusny, Alexander Grünberger, Christopher Probst, Wolfgang Wiechert, Dietrich Kohlheyer, and Andreas Schmid. Technical bias of microcultivation environments on single-cell physiology. *Lab on a chip*, 15(8):1822–1834, 2015.

[10] C Wyatt Shields IV, Catherine D Reyes, and Gabriel P López. Microfluidic cell sorting: a review of the advances in the separation of cells from debulking to rare cell isolation. *Lab on a Chip*, 15(5):1230–1249, 2015.

[11] Valentine Svensson, Roser Vento-Tormo, and Sarah A Teichmann. Exponential scaling of single-cell rna-seq in the past decade. *Nature protocols*, 13(4):599–604, 2018.

[12] Xiannian Zhang, Tianqi Li, Feng Liu, Yaqi Chen, Jiacheng Yao, Zeyao Li, Yanyi Huang, and Jianbin Wang. Comparative analysis of droplet-based ultra-high-throughput single-cell rna-seq systems. *Molecular cell*, 73(1):130–142, 2019.

[13] Vanessa M Peterson, Kelvin Xi Zhang, Namit Kumar, Jerelyn Wong, Lixia Li, Douglas C Wilson, Renee Moore, Terrill K McClanahan, Svetlana Sadekova, and Joel A Klappenbach. Multiplexed quantification of proteins and transcripts in single cells. *Nature biotechnology*, 35(10):936, 2017.

[14] Howard M Shapiro. *Practical flow cytometry*. John Wiley & Sons, 2005.

[15] Zach B Bjornson, Garry P Nolan, and Wendy J Fantl. Single-cell mass cytometry for analysis of immune system functional states. *Current opinion in immunology*, 25(4):484–494, 2013.

[16] Sean C Bendall, Erin F Simonds, Peng Qiu, D Amir El-ad, Peter O Krutzik, Rachel Finck, Robert V Bruggner, Rachel Melamed, Angelica Trejo, Olga I Ornatsky, et al. Single-cell mass cytometry of differential immune and drug responses across a human hematopoietic continuum. *Science*, 332(6030):687–696, 2011.

[17] Yacine Bounab, Klaus Eyer, Sophie Dixneuf, Magda Rybczynska, Cécil Chauvel, Maxime Mistretta, Trang Tran, Natan Aymerich, Guilhem Chenon, Jean-Francois Llitjos, Fabienne Venet, Guillaume Monneret, Iain Gillespie, Pierre Cortez, Virginie Moucadel, Alexandre Pachot, Alain Troesch, Julien Leissner, Jérôme Bibette, Cyril Guyard, Jean Baudry, Andrew D Griffiths, and Christophe Védrine. Dynamic single-cell phenotyping of immune cells.

[18] Klaus Eyer, Phillip Kuhn, Conni Hanke, and Petra S Dittrich. A microchamber array for single cell isolation and analysis of intracellular biomolecules. *Lab on a Chip*, 12(4):765–772, 2012.

[19] Alan Dove. Drug screening—beyond the bottleneck. *Nature biotechnology*, 17(9):859–863, 1999.

[20] Linas Mazutis, John Gilbert, W Lloyd Ung, David A Weitz, Andrew D Griffiths, and John A Heyman. Single-cell analysis and sorting using droplet-based microfluidics. *Nature protocols*, 8(5):870, 2013.

[21] Jenifer Clausell-Tormos, Diana Lieber, Jean-Christophe Baret, Abdeslam El-Harrak, Oliver J Miller, Lucas Frenz, Joshua Blouwolff, Katherine J Humphry, Sarah Köster, Honey Duan, et al. Droplet-based microfluidic platforms for the encapsulation and screening of mammalian cells and multicellular organisms. *Chemistry & biology*, 15(5):427–437, 2008.

[22] Wendy Anne Boivin, Dawn Michelle Cooper, Paul Ryan Hiebert, and David James Granville. Intracellular versus extracellular granzyme b in immunity and disease: challenging the dogma. *Laboratory investigation*, 89(11):1195–1220, 2009.

[23] Christof Wagner, Christof Iking-Konert, Birgit Denefleh, Sabine Stegmaier, Friederike Hug, and Hansch G Maria. Granzyme b and perforin: constitutive expression in human polymorphonuclear neutrophils. *Blood*, 103(3):1099–1104, 2004.

[24] Won-Jung Kim, Ho Kim, Kyoungho Suk, and Won-Ha Lee. Macrophages express granzyme b in the lesion areas of atherosclerosis and rheumatoid arthritis. *Immunology letters*, 111(1):57–65, 2007.

[25] Cornelia M Tschopp, Nicole Spiegl, Svetlana Didichenko, Werner Lutmann, Peter Julius, J Christian Virchow, C Erik Hack, and Clemens A Dahinden. Granzyme b, a novel mediator of allergic inflammation: its induction and release in blood basophils and human asthma. *Blood*, 108(7):2290–2299, 2006.

[26] Marie-Clotilde Rissoan, Thomas Duhen, Jean-Michel Bridon, Nathalie Bendriss-Vermare, Catherine Péronne, Blandine de Saint Vis, Francine Briere, and Elizabeth EM Bates. Subtractive hybridization reveals the expression of immunoglobulinlike transcript 7, eph-b1, granzyme b, and 3 novel transcripts in human plasmacytoid dendritic cells. *Blood*, 100(9):3295–3303, 2002.

[27] Dipanjan Chowdhury and Judy Lieberman. Death by a thousand cuts: granzyme pathways of programmed cell death. *Annu. Rev. Immunol.*, 26:389–420, 2008.

[28] SP Cullen and SJ Martin. Mechanisms of granule-dependent killing. *Cell Death & Differentiation*, 15(2):251–262, 2008.

[29] John H Russell and Timothy J Ley. Lymphocyte-mediated cytotoxicity. *Annual review of immunology*, 20(1):323–370, 2002.

[30] Susan A Weston and Christopher R Parish. New fluorescent dyes for lymphocyte migration studies: analysis by flow cytometry and fluorescence microscopy. *Journal of immunological methods*, 133(1):87–97, 1990.

[31] Mathias T Rosenfeldt, Michael Valentino, Salvatore Labruzzo, Lesley Scudder, Maria Pavlaki, Jian Cao, Jeffrey Vacirca, Wadie F Bahou, and Stanley Zucker. The organomercurial 4-aminophenylmercuric acetate, independent of matrix metalloproteinases, induces dose-dependent activation/inhibition of platelet aggregation. *Thrombosis and haemostasis*, 93(02):326–330, 2005.

[32] C Grierson, D Miller, P LaPan, and J Brady. Utility of combining mmp-9 enzyme-linked immunosorbent assay and mmp-9 activity assay data to monitor plasma enzyme specific activity. *Analytical biochemistry*, 404(2):232–234, 2010.

[33] R.L. Lundblad. *Chemical Reagents for Protein Modification*. CRC Press, 2014.

[34] Sudha B Singh and Henry C Lin. Autophagy counters lps-mediated suppression of lysozyme. *Innate immunity*, 23(6):537–545, 2017.

[35] Kyra J Cowan and Kenneth B Storey. Freeze-thaw effects on metabolic enzymes in wood frog organs. *Cryobiology*, 43(1):32–45, 2001.

[36] Piet Borst, Raymond Evers, Marcel Kool, and Jan Wijnholds. The multidrug resistance protein family. *Biochimica et Biophysica Acta (BBA)-Biomembranes*, 1461(2):347–357, 1999.